Modulational instability and pattern formation in discrete dissipative systems

Alidou Mohamadou[1,2] and Timoléon Crépin Kofané[1,3]
[1]*Laboratory of Mechanic, Department of Physics, Faculty of Science, University of Yaoundé I, P.O. Box 812, Yaoundé, Cameroon*
[2]*Condensed Matter Laboratory, Department of Physics, Faculty of Science, University of Douala, P.O. Box 24157, Douala, Cameroon*
[3]*Max-Planck-Instiut for the Physics of Complex Systems, Noethnitzer Strasse 38, D-01187 Dresden, Germany*
(Received 26 September 2005; published 13 April 2006)

We report in this paper the study of modulated wave trains in the one-dimensional (1D) discrete Ginzburg-Landau model. The full linear stability analysis of the nonlinear plane wave solutions is performed by considering both the wave vector (**q**) of the basic states and the wave vector (**Q**) of the perturbations as free parameters. In particular, it is shown that a threshold exists for the amplitude and above this threshold, the induced modulational instability leads to the formation of ordered and disordered patterns. The theoretical findings have been numerically tested through direct simulations and have been found to be in agreement with the theoretical prediction. We show numerically that modulational instability is also an indicator of the presence of discrete solitons as were early predicted to exist in Ginzburg-Landau lattices.

DOI: 10.1103/PhysRevE.73.046607 PACS number(s): 05.45.Yv, 42.65.Tg, 89.75.Kd, 89.75.Fb

I. INTRODUCTION

In recent years, the topic of waves in discrete dissipative systems has received considerable attention due to the diversity of their numerous applications in physical and biological sciences. The structure of such systems implies that their dynamics is the result of an interaction between individual dynamical entities. Molecular chain [1], Josephson junction [2], and photonic structures (in arrays of coupled nonlinear optics waveguides [3] and in a nonlinear photonic crystal structure [4]) are examples referred to as coupled oscillators [5]. Photonic crystals, which are artificial microstructures having photonic band gaps [6], can be used to precisely control propagation of optical pulses and beams [7]. They are very useful for optical components such as waveguides, couplers, cavities, and optical computers. It is possible to make discrete waveguides using crystals. Stationary solutions to these systems can frequently be found by using both analytical and numerical methods. One of the fundamental problems left is to check these solutions against their stability, which is essential from a basic point of view as well as for potential applications; see, e.g., [8–14], and references therein. Different kinds of instability may lead to such phenomena as bistability [15], self-oscillation, and the formation of static or moving patterns [16]. A prominent example is modulational instability (MI). Modulational instability is the outcome of interplay between nonlinearity and dispersive/diffraction effects. It is a symmetry-breaking instability so that a small perturbation on top of a constant amplitude background experiences exponential growth and this leads to wave breakup in either space or time. Since this disintegration typically occurs in the same parameters region where bright solitons are observed, MI is considered to some extent, a precursor to soliton formation [14]. A general formulation of the problem of nonlinear wave propagation via fundamental sets of equations, such as, for example, the Maxwell or Navier-Stokes equations, is a very demanding task even for modern computers. Therefore a number of simplified models have been introduced which approximately describe either propagation of the wave itself, e.g., the Korteweg–de Vries (KdV) equation [17], or propagation of a slowly varying wave envelope, e.g., the nonlinear Schrödinger (NLS) equation [17] or the complex Ginzburg-Landau (CGL) equation [18]. It was recognized much later that the condition for MI would be significantly modified for discrete settings relevant to, for instance, the local denaturation of DNA [19] or coupled arrays of optical waveguides [20]. In the latter case, a relevant model is the discrete nonlinear Schrödinger equation (DNLS) [21], and its MI conditions were discussed in [22]. Moreover, it has been shown that recurrence phenomena and the existence of localized excitations in discrete systems can be attributed to MI of stationary solutions of the respective nonlinear equations [22,23]. It turned out that a particular feature of these systems consists in the critical dependence of both the MI gain (instability increment) and the domain of MI on the wave vector of the stationary solution.

The complex Ginzburg-Landau equation is known to play a ubiquitous role in science. This equation is encountered in several diverse branches of physics, such as, for example, in superconductivity and superfluidity, nonequilibrium fluid dynamics and chemical systems, nonlinear optics, Bose-Einstein condensates, and quantum field theories [5,18,23–26]. Very often used in fluid mechanics as a phenomenological equation, the CGL equation and its different forms were analytically derived in various applications (see Ref. [27], for instance) where it appears as an amplitude equation for rapidly oscillating wave propagating in nonlinear medium. In addition to the well-studied continuous CGL equation, the discretized forms of the CGL equation have also been considered in the literature. Semiconductor laser arrays [28], vortex line dynamics [29], and the study of coupled wakes [30] have been described by discrete CGL (DCGL) lattices. In these latter examples, the oscillation of each isolated cell (each vortex or wakes) obeys a Landau equation which is the normal form of the Hopf bifurcation that creates each oscillator. The global behavior of the vortex or wake arrays can consequently be described by the dynam-

ics of coupled Hopf oscillators. The CGL equation which describes the small and slowly varying amplitude and phase of a mode that bifurcates via an oscillatory instability from a homogeneous basis states is most useful for supercritical bifurcations. For subcritical bifurcation, one expects blow up of the solutions which can only be avoided by adding at least a fifth-order stabilizing term. Efremidis and Christodoulides have studied the DCGL equation with a quintic nonlinearity [31]. They found that discrete solitons are possible in Ginzburg-Landau lattices. As a result of discreteness, the complex cubic-quintic Ginzburg-Landau (CCQGL) equation exhibits several features that have no counterparts in either the continuous limit or in other conservative discrete models. Soto-Crespo *et al.* [32] have studied the stability of soliton solutions of the DCCQGL equations. Thereafter, Atai and Malomed [33] have investigated the existence and stability of solitons in an optical waveguide equipped with a Bragg grating (BG) in which nonlinearity contains both cubic and quintic terms. They have found analytically two different families of zero-velocity solitons, which are separated by a border at which solitons do not exist. Ravous *et al.* [34] studied the discrete analog of the complex cubic Ginzburg-Landau equation having pattern formation in mind. In particular, they studied plane wave instability in such systems. Until now, studies on MI have been mostly directed to nonlinear physics of conservative systems [25,35]. We deal below with the phenomenon of MI in nonconservative system, viz., the DCCQGL equation.

Very recently, it has been shown that discrete solitons are possible in Ginzburg-Landau models [31]. In view of what was said above, our aim in this paper is to study MI for plane waves across the non-conservative system. Therefore we derive analytical expression for the domain of existence as well as the gain of MI of plane wave. This domain leads to the generation of pulse trains with high repetition rate, i.e., solitons.

The rest of this paper is structured as follows. In Sec. II, we present the mathematical framework and our analytical results. We then continue in Sec. III where we investigate numerically the accuracy of the analytical results. In Sec. IV, we investigate the different wave pattern formations that the nonlinear plane waves may display. Finally, in Sec. V, we summarize our results and present our conclusions.

II. SETUP AND ANALYTICAL CONSIDERATIONS

Many nonequilibrium phenomena such as phase transition and wave propagation can be described by the DCGL lattices [5,28–34]

$$i\dot{u}_n - i\epsilon u_n + \alpha(u_{n+1} + u_{n-1}) + p|u_n|^2 u_n + C|u_n|^4 u_n = 0, \quad (1)$$

where $p=p_r+ip_i$, $C=C_r+iC_i$, $\alpha=\alpha_r+i\alpha_i$, ϵ is a real parameter, and $\dot{u}_n=du_n/dz$. Physically, the discrimination in Eq. (1) occurs by applying the tight binding approximation (or coupled mode theory) [28,36]. The original, periodic in space, continuous system is expanded in local modes, whose amplitudes are described by the corresponding discrete model. In Eq. (1), α_r accounts for the energy tunneling between adjacent elements of the lattice, while its imaginary part stands for gain (losses) due to coupling. The real parts of p and C represent the strength of the cubic and quintic nonlinearity of the system, while ϵ, p_i, C_i are the linear and nonlinear gain (loss) coefficients. The DCCQGL equation can describe the dynamics of an open Bose-Einstein condensate. In this case, the lattice potential is created by the interferences of two standing waves [37] and, thus, solitons of the DNLS type are known to exist [38]. Within the context of nonlinear optics, the DCGL equation also arises in the description of semiconductor laser arrays [28], where the quintic term can account for the gain and nonlinearity saturation of the lasing medium.

The system has the nonlinear plane waves solutions defined by $u_n(z)=u_0\exp[i(qna-\omega z)]$. This solution leads to the nonlinear dispersion relation

$$\omega + 2\alpha_r\cos(qa) + (p_r + C_r|u_0|^2)|u_0|^2 = 0,$$

$$|u_0|^2 = \{-p_i \pm \sqrt{p_i^2 + 4C_i[\epsilon - 2\alpha_i\cos(qa)]}\}/2C_i, \quad (2)$$

where ω is the angular frequency, q the wave vector, and u_0 a nonzero initial wave amplitude. To find under which conditions isolated pulses could be formed during the evolution of wave in the system, we investigate the time evolution of a perturbed nonlinear wave of the form

$$u_n(z) = [u_0 + b_n(z)]\exp[i\theta_n(z)], \quad (3)$$

where the perturbation $b_n(z)$ is complex and is assumed to be infinitesimal in magnitude in comparison with that of the amplitude of the carrier wave. Next, we insert the above solution into Eq. (1), using Eq. (2) and keeping only linear terms in the perturbation quantity, we obtain the following first-order differential-difference equation for the perturbation $b_n(t)$:

$$i\dot{b}_n + \alpha(b_{n+1} + b_{n-1} - 2b_n)\cos(qa) + i\alpha(b_{n+1} - b_{n-1})\sin(qa) + (p + 2C|u_0|^2)|u_0|^2(b_n + b_n^*) = 0, \quad (4)$$

where the asterisk denotes complex conjugation. The solution of Eq. (4) can be written as a combination of progressive and progressive waves of the form

$$b_n(Q) = \sum_Q b_1(Q)e^{i(Qma-\Omega z)} + \sum_Q b_2^*(Q)e^{-i(Qna-\Omega^* z)}, \quad (5)$$

where Q and Ω stand for the wave vector and the frequency of the linear modulation, respectively. Substitution of (5) into (4) yields a linear homogeneous system for b_1 and b_2. The coefficients of the 2×2 matrix (m_{ij}) are given by

$$m_{11} = 2i\alpha[\cos(Qa) - 1]\cos(qa) - 2i\alpha\sin(qa)\sin(Qa) + i(p + 2C|u_0|^2)|u_0|^2, \quad (6)$$

$$m_{12} = i(p + 2C|u_0|^2)|u_0|^2, \quad (7)$$

$$m_{21} = -i(p^* + 2C^*|u_0|^2)|u_0|^2, \quad (8)$$

$$m_{22} = -2i\alpha^*[\cos(Qa)-1]\cos(qa) - 2i\alpha^* \sin(qa)\sin(Qa) - i(p^* + 2C^*|u_0|^2)|u_0|^2. \quad (9)$$

The linear homogeneous system for b_1 and b_2 has a nontrivial solution if its determinant vanishes. This gives the condition

$$\Omega^2 + i(m_{11}+m_{22})\Omega + m_{12}m_{21} - m_{11}m_{22} = 0. \quad (10)$$

Thus, to obtain explicitly the criterion, the roots of the above dispersion relation have to be derived. The discriminant (Δ) of Eq. (10) can be written as $\Delta = X + iY$, where

$$\begin{aligned} X = {} & 4\{2\alpha_i[\cos(Q)-1]\cos(q)\} + p_t|u_0|^2 + 2C_i|u_0|^4 \\ & - 4[\alpha_r \sin(Q)\sin(q)]^2 + 4|\alpha|^2[\sin(Q)\sin(q)]^2 \\ & - 4|\alpha|^2\{[\cos(Q)-1]\cos(q)\}^2 + |u_0|^4[|p|^2 + 4|C|^2|u_0|^4 \\ & + 4(p_rC_r + p_iC_i)|u_0|^2] - |p|^2|u_0|^4 - 4|C|^2|u_0| - 4(\alpha_r p_r \\ & + \alpha_i p_i)|u_0|^2[\cos(Q)-1]\cos(q) - 8(\alpha_r C_r + \alpha_i C_i) \\ & \times |u_0|^4 \sin(Q)\sin(q) - 4(p_rC_r + p_iC_i)|u_0|, \end{aligned} \quad (11)$$

$$\begin{aligned} Y = {} & 8\alpha_r \sin(q)\sin(Q)\{2\alpha_r[\cos(Q)-1]\cos(q) + p_i|u_0|^2 \\ & + 2C_i|u_0|^4\} + 4(\alpha_i p_r - \alpha_r p_i)|u_0|^2 \sin(q)\sin(Q) \\ & + 8(\alpha_i C_r - \alpha_r C_i)|u_0|^2 \sin(q)\sin(Q). \end{aligned} \quad (12)$$

Next, we label by Ω_1 and Ω_2 the general solution roots of Eq. (10), viz.,

$$\Omega_1 = f + ig + \sqrt{\Delta}, \quad (13)$$

$$\Omega_2 = f + ig - \sqrt{\Delta}, \quad (14)$$

in which

$$f = -2\{2\alpha_i[\cos(Q)-1]\cos(q) + p_i|u_0|^2 + 2C_i|u_0|^4\} \quad (15)$$

and

$$g = -2\alpha_r \sin(Q)\sin(q).$$

If we introduce the notation $h_1 = \sqrt{\frac{1}{2}(X + \sqrt{X^2+Y^2})}$ and $h_2 = \sqrt{\frac{1}{2}(-X + \sqrt{X^2+Y^2})}$, where h_1 and h_2 are the roots of Δ, from Eqs. (13) and (14) we write

$$\Omega_1 = f + ig + h_1 - ih_2 = (f + h_1) - i(g - h_2), \quad (16)$$

$$\Omega_2 = f + ig - h_1 + ih_2 = (f - h_1) + i(g + h_2). \quad (17)$$

Here, the two cases are possible related each to the sign of Y. So the expressions (16) and (17) are established for the case $Y < 0$. In the case $Y > 0$, the roots of Eq. (10) take the form

$$\Omega_1' = f + ig - h_1 - ih_2 = (f - h_1) + i(g - h_2), \quad (18)$$

$$\Omega_2' = f + ig + h_1 + ih_2 = (f + h_1) + i(g + h_2),$$

and lead to solutions with the same asymptotic behavior as those obtained from Eqs. (13) and (14). Since the frequency Ω is complex the stability of the system is determined by the imaginary part of Ω. The behavior of the perturbation (5) through the system is well understood by introducing Eq. (16) into relation (5). This operation gives

$$b_n(Q) = \sum_Q b_1(Q) e^{i[Qna - (f+h_1)z]} e^{-(g-h_2)z} + \sum_Q b_2^*(Q) e^{-i[Qna-(f+h_1)z]} e^{-i(g-h_2)z}. \quad (19)$$

The general solution of the system (4) initially formulated in Eq. (5) appears as a superposition of terms having the time dependence ($e^{-(g-h_2)z}$), which is related to the amplitude of the perturbation as one can see in Eq. (19). Therefore the asymptotic behavior of the extended nonlinear plane wave is determined by the sign of the quantity $g - h_2$, which corresponds to the imaginary part of Ω_1. Since the coefficient h_2 is always positive, the inequality $g - h_2 < g + h_2$ holds. The difference $h_2 - g$ is always positive if $g < 0$, and then the solution (5) increases exponentially when the time z tends to infinity. In this case, the perturbation grows up, i.e., the system remains unstable under modulation. On the other hand, if $g > 0$ the asymptotic behavior of Eq. (5) will depend on the sign of $g - h_2$. At this level, we shall distinguish two cases.

(1) First of all, if $h_2 - g > 0$, we see that the imaginary part of Ω is negative, $\mathrm{Im}(\Omega) < 0$, and the system is said to be modulationally unstable, due to the fact that solution (5) diverges without limit as the time z increases. To be more explicit, we can write the form of the difference $g - h_2$ as

$$\begin{aligned} g - h_2 = g - \Bigg(& \frac{1}{2}(4\{2\alpha_i[\cos(Q)-1]\cos(q) + p_i|u_0|^2 \\ & + 2q_i|u_0|^4\}^2 - 4[\alpha_r \sin(q)\sin(Q)]^2 - |p|^2|u_0|^4 \\ & + |u_0|^4[|p|^2 + 4|C|^2|u_0|^4 + 4(p_rC_r + p_iC_i)|u_0|^2] \\ & + 4|\alpha|^2[\sin(q)\sin(Q)]^2 - 4|C|^2|u_0|^8 - 8(\alpha_r q_r + \alpha_i q_i) \\ & \times |u_0|^4 \sin(q)\sin(Q) - 4(p_rC_r + p_iC_i)|u_0|^6 \\ & + \sqrt{X^2+Y^2} - 4(\alpha_r p_r + \alpha_i p_i)|u_0|^2[\cos(Q)-1]\cos(q) \\ & - 4|\alpha|^2\{[\cos(Q)-1]\cos(q)\}^2) \Bigg)^{1/2}. \end{aligned} \quad (20)$$

When we remove positive quantities in Eq. (20), we obtain the following inequality:

$$\begin{aligned} g - h_2 \leqslant g - \Bigg(& \frac{1}{2}(-4[\alpha_r \sin(q)\sin(Q)]^2 - |p|^2|u_0|^4 \\ & - 4|\alpha|^2\{[\cos(Q)-1]\cos(q)\}^2 - |p|^2|u_0|^4 - 8(\alpha_r C_r \\ & + \alpha_i C_i)|u_0|^4 \sin(q)\sin(Q) - 4(p_rC_r + p_iC_i)|u_0|^6 \\ & - 4|C|^2|u_0|^8 - 4(\alpha_r p_r + \alpha_i p_i)|u_0|^2[\cos(Q)-1]\cos(q) \\ & + 4(p_rC_r + p_iC_i)|u_0|^6) \Bigg)^{1/2}. \end{aligned} \quad (21)$$

We have said above that this quantity which represents the imaginary part of the frequency must be negative. Knowing that g is a positive constant, we have

$$\begin{aligned} & -(\alpha_r p_r + \alpha_i p_i)|u_0|^2\{[\cos(Q)-1]\cos(q)\} - 2(\alpha_r C_r + \alpha_i C_i) \\ & \times [\sin(q)\sin(Q)]|u_0|^4 > 2g^2 + 4[\alpha_r \sin(q)\sin(Q)]^2 \\ & + |p|^2|u_0|^4 + 4|\alpha|^2\{[\cos(Q)-1]\cos(q)\}^2 + |p|^2|u_0|^4 \end{aligned}$$

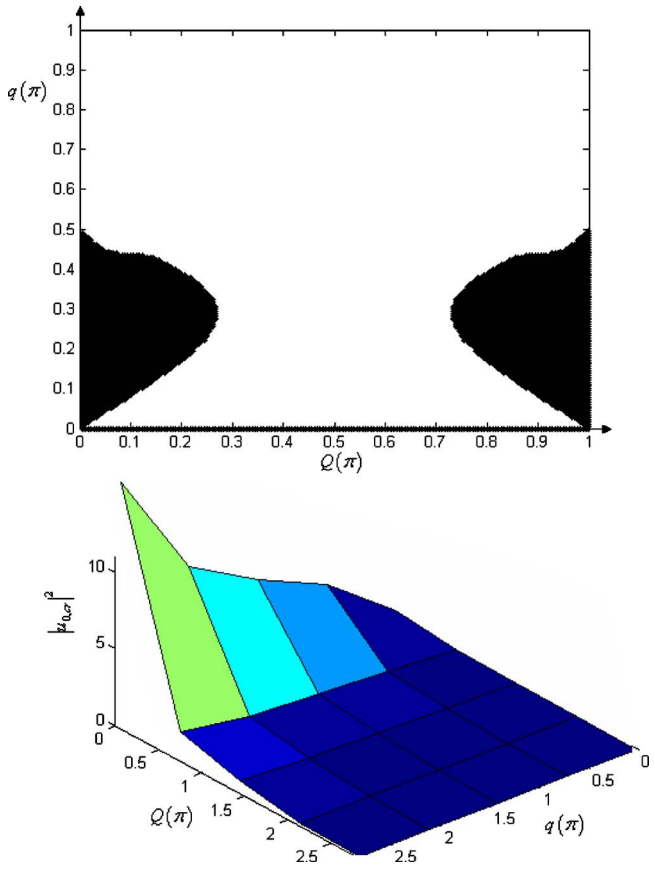

FIG. 1. (Color online) $\alpha=3.0-3.25i$, $p=0.50-2.25i$, $C=-0.25+0.30i$, $\varepsilon=1.0$. (a) Instability-stability regions on the (q,Q) plane. (b) Threshold amplitude.

$$+4|C|^2|u_0|^8>0, \tag{22}$$

and we write

$$-(\alpha_r p_r+\alpha_i p_i)\{[\cos(Q)-1]\cos(q)\}-2(\alpha_r C_r+\alpha_i C_i)\times[\sin(q)\sin(Q)]|u_0|^2>0. \tag{23}$$

Equation (23) defines the condition under which an initial wave previously introduced in the system lead to the break up of uniform disturbances into modulated structures. Because of the discreteness of the lattice, the wave vectors $\mathbf{q}$ and $\mathbf{Q}$ that differ by 2π correspond to the same wave. Thus we can restrict our study to the first Brillouin zone $[-\pi,\pi]$. Finally, we consider $[0,\pi]$ since only the direction of propagation is changing for $-\mathbf{q}$ and $-\mathbf{Q}$. In contrast to the analogous condition for a continuous system, the stability condition depends on the wave vector $\mathbf{q}$ and the perturbation wave vector $\mathbf{Q}$. This is specific to the discretized complex Ginzburg-Landau equation. Figure 1(a) shows the different instability zones in the $(\mathbf{q},\mathbf{Q})$ plane, for the parameters $\alpha_r=3.0$, $\alpha_i=-3.25$, $p_r=0.50$, $p_i=-2.25$, $C_r=-0.25$, $C_i=0.30$, and $\varepsilon=1.0$. The dark areas correspond to a region where nonlinear plane waves are unstable with respect to modulation of any wave vector $\mathbf{Q}$. Everywhere there exists a wave vector $\mathbf{Q}$ which destabilizes the nonlinear plane wave considered. In particular, note that there is an interval in $\mathbf{q}$ (here, $0.55<q<1$) in which every nonlinear wave is stable whatever its wave vector $\mathbf{Q}$. We have also noted that the area of instability depends on the quintic coefficients. Region of instability increases when C_r becomes weaker ($C_r<0$) or when one increases the value of the coefficient $C_i(C_i>0)$, but is reduced when the value of the parameters $C_r(C_r>0)$ decreases. In most cases, a criterion for instability does not depend on the amplitude of monochromatic wave. But for the DCCQGL equation, the criterion indicated depends on the amplitude $|u_0|^2$. This fact allows us to determine the threshold amplitude of an unstable monochromatic wave for a given wave vector, viz.,

$$|u_0|^2>|u_{0,c}|^2=-\frac{(\alpha_r p_r+\alpha_i p_i)\{[\cos(Q)-1]\cos(q)\}}{2(\alpha_r C_r+\alpha_i C_i)[\sin(q)\sin(Q)]}. \tag{24}$$

From Eq. (24), we see that a plane wave will be unstable to any modulation provided that the initial amplitude $|u_0|^2$ exceeds the threshold $|u_{0,c}|^2$ defined by relation (24). The corresponding threshold amplitude ($|u_{0,c}|^2$) for the parameters of Fig. 1(a) is depicted in Fig. 1(b) as a function of the perturbation wave number Q and the initial wave number q of the carrier wave. We observe that, the more discreteness effects are important ($Q\to Q_{\max}=\pi$ and $q\to q_{\max}=\pi$), the higher the necessary amplitude leading to MI.

(2) Second, from the above calculations, we can deduce that, when the imaginary part of Ω is positive $g-h_2>0$ [$\mathrm{Im}(\Omega)>0$], we obtain the following criterion:

$$-(\alpha_r p_r+\alpha_i p_i)\{[\cos(Q)-1]\cos(q)\}-2(\alpha_r C_r+\alpha_i C_i)\times[\sin(q)\sin(Q)]|u_0|^2<0. \tag{25}$$

This result means that Stokes waves which verify (25) are stable under modulation.

It is interesting to compare the MI of the DGL equation with results on MI of the continuous GL equation. The connection between the DGL equation, and the continuous GL equation is established by applying a Taylor series expansion and, as a result, Eq. (1) can be approximated by the continuous GL equation [39]. Then, the stability criterion can be obtained from relation (23) by considering the limiting case of long-wavelength limit for the modulation wave which is assumed in the semidiscrete approximation, i.e., Q and q are small ($Q\ll 1$ and $q\ll 1$),

$$(\alpha_r p_r+\alpha_i p_i)\frac{Q^2}{2}-2(\alpha_r C_r+\alpha_i C_i)qQ|u_0|^2>0. \tag{26}$$

This result is in accordance with previous study of MI made on continuous systems [40]. Moreover, relation (23) can be viewed as the discrete Lange and Newell's criterion [41].

III. NUMERICAL RESULTS

The results presented in the previous section were deduced from a linear stability analysis. But as it is well known, the linear stability analysis seems to be limited because it can only detect the onset of instability, but it does not tell us anything about the behavior of the system when

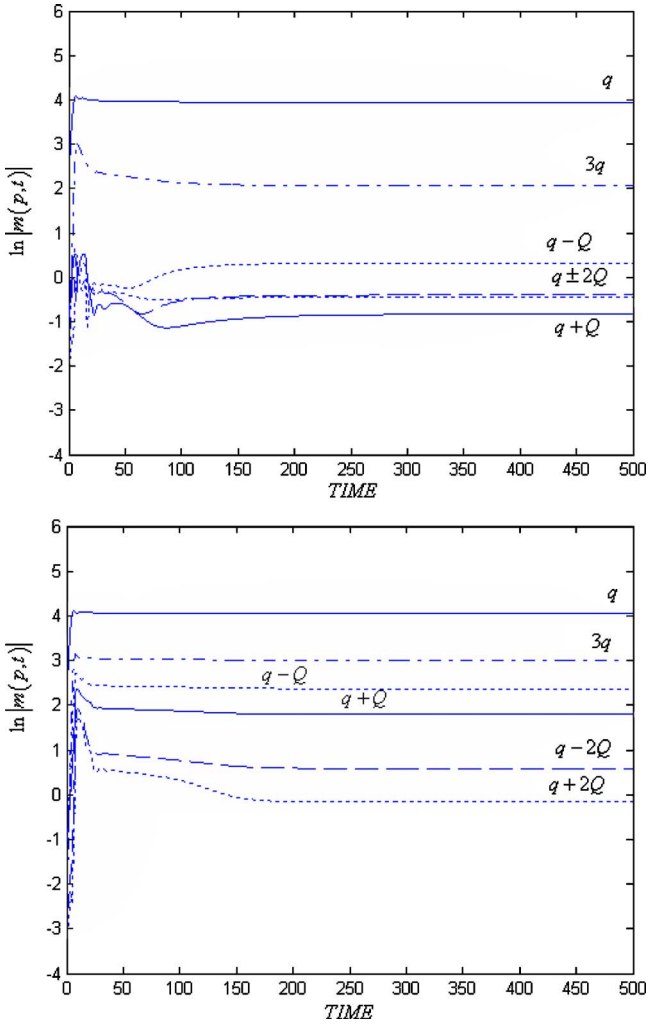

FIG. 2. (Color online) Time evolution of the amplitude of the main Fourier transform components. A logarithmic scale is used for ordinate. (a) The carrier wave $q=3\pi/32$ is modulated by a small-amplitude wave vector $Q=\pi/8$. (b) The carrier wave $q=\pi/32$ is modulated by a small-amplitude wave vector $Q=3\pi/16$.

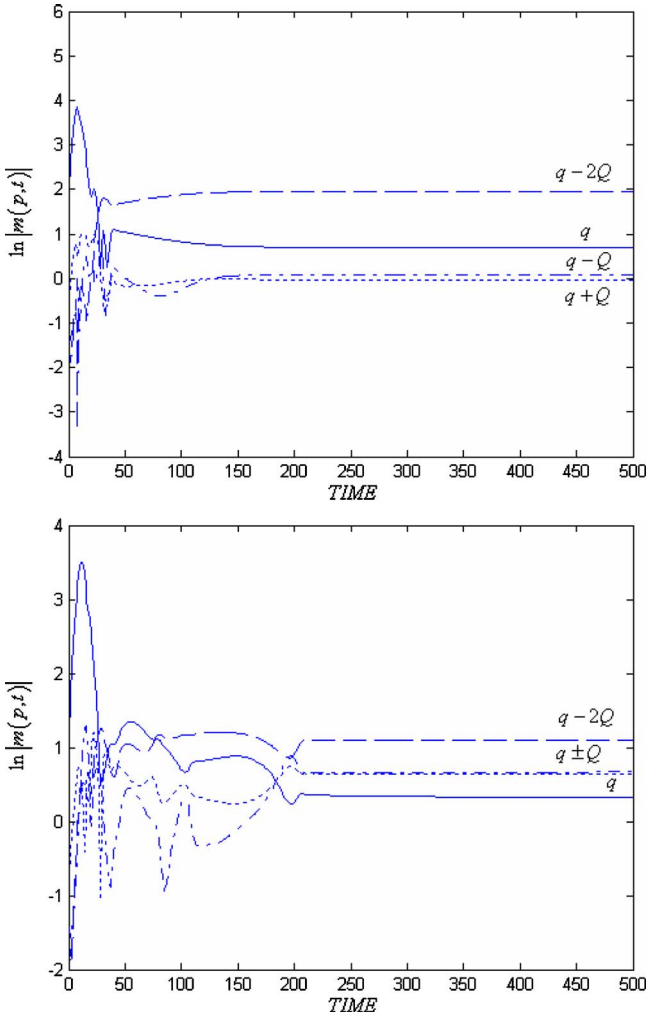

FIG. 3. (Color online) Time evolution of the amplitude of the main Fourier transform components. A logarithmic scale is used for ordinate. (a) The carrier wave $q=5\pi/16$ is modulated by a small-amplitude wave vector $Q=3\pi/32$. (b) The carrier wave $q=7\pi/16$ is modulated by a small-amplitude wave vector $Q=\pi/16$.

the instability grows after a long time. That is why in this section, we present the results of a numerical experiment in the DCCQGL equation. So said, the validity of the analytical results obtained from the linear stability analysis of the extended nonlinear waves is discussed for a variety of equation parameters. The influence of the cubic-quintic term on the stability is also discussed. Our numerical calculations have been done through a computer-simulation program in order to make contact with the analytical prediction at short time as well as to examine longer time dynamics of the nonlinear system which is subject to MI. A fourth-order Runge-Kutta scheme is used to integrate Eq. (1). Most of the simulations are performed with a chain of 128 sites with periodic boundary conditions; the wave vectors q and Q are defined modulo 2π in the lattice and chosen in the form $q=2\pi p/N$ and $Q=2\pi P/N$ where p and P are integers lower than $N/2$.

The initial conditions, which are typically at time $t=0$, are obtained by using a complex wave function that can be written as

$$u_n(t) = u_n^{re}(t) + iu_n^{im}(t) \tag{27}$$

Here, the upper indexes (re) and (im), stand for the real and imaginary part, respectively. We start from a solution of the DCCQGL equation as a plane wave of wave vector q with an amplitude which is perturbed by a modulation plane wave with wave vector Q since we are interested in MI. Thus initially, in our numerical simulation, the real and the imaginary part of the wave function of the plane wave are coherently modulated in the form

$$u_n^{re}(0) = [u_0 + \eta\cos(nQ)]\cos(nq), \tag{28a}$$

$$u_n^{im}(0) = [u_0 + \eta\cos(nQ)]\sin(nq). \tag{28b}$$

This initial condition is therefore a modulated plane wave with amplitude u_0, that is derived from the preceding section [Eq. (2)] and the modulation amplitude $\eta \ll u_0$. So, using the initial condition given in Eq. (28) has revealed that in this simple coherent modulation form of the amplitude, this ini-

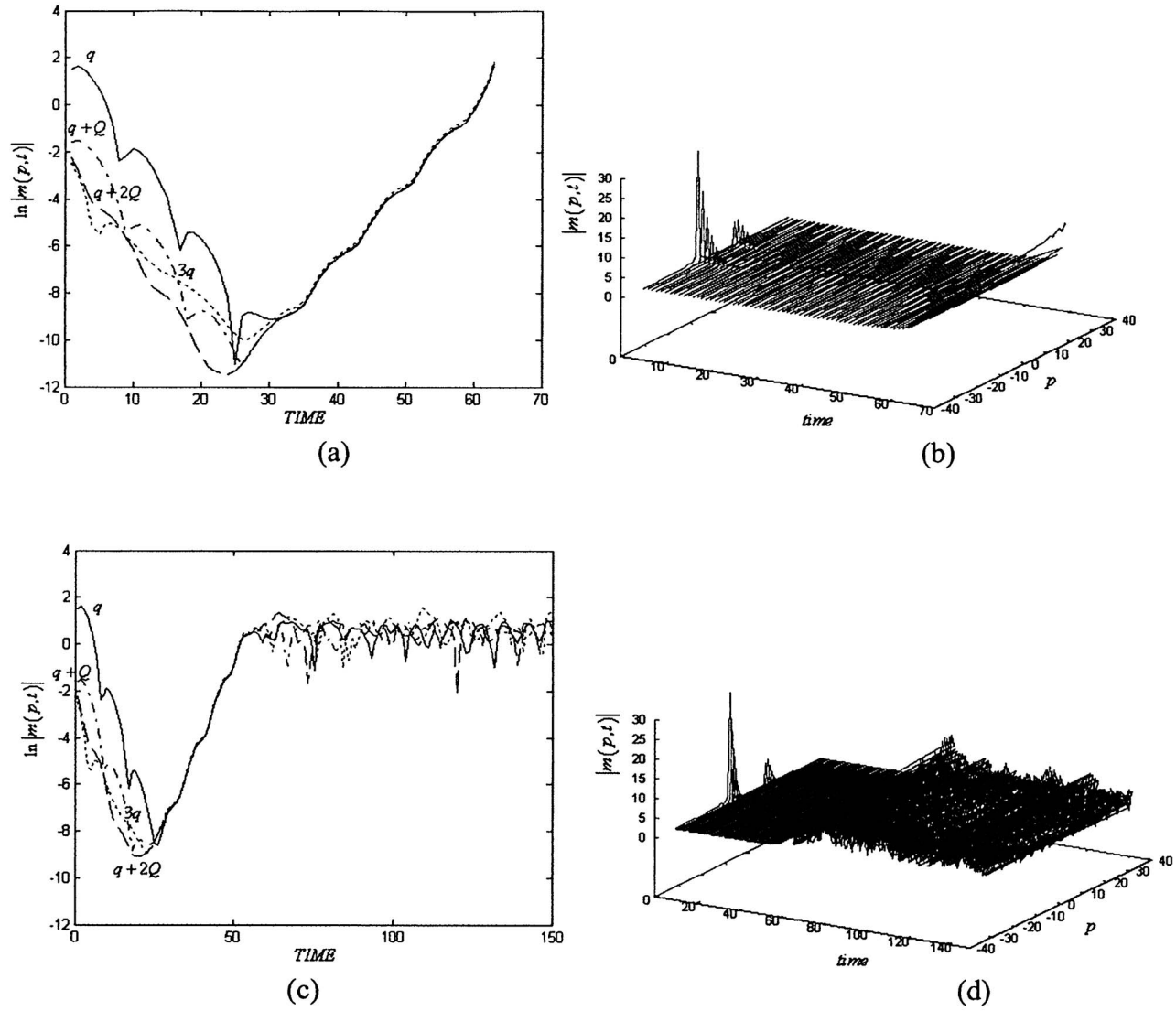

FIG. 4. Influence of the quintic term. (a) The model parameters are $\alpha=1.5+0.725i$, $p=0.150-0.125i$, $\varepsilon=-0.250$; the carrier wave $q=\pi/8$ is modulated by a small-amplitude wave vector $Q=\pi/16$. The system presents a chaotic behavior. (b) Time evolution of the complete Fourier spectrum. (c) The quintic term $C=-0.3+0.30i$ is used to stabilize the amplitude of the combination modes. (d) Time evolution of the complete Fourier spectrum.

tial condition allows us to study the response of the system separately for each modulation wave vector. Finally, we will study the behavior of this wave with the help of the discrete spatial Fourier transform of the $u_n(t)$:

$$m(p,t) = \sum_{n=0}^{N-1} u_n(t) e^{i(2\pi np/N)}. \tag{29}$$

A. Stability

We will restrict ourselves to the behavior of the system for short times, and we will show that the results are in very good agreement with the theoretical predictions deduced from Eq. (23) if we take into account that the nonlinearity itself could create additional modulation. Indeed, an initial linear wave $u_n(0)=A\cos(nq)$ chosen as the initial condition will immediately create a nonlinear component $\cos^3(nq)$ for the cubic nonlinearity as

$$u_n(0) = A\cos(nq) + B\cos^3(nq)$$
$$= \left(A + \frac{B}{2}[1+\cos(n2q)]\right)\cos(nq). \tag{30}$$

We can see that a modulation with wave vector $Q=2q$ is immediately generated by the cubic nonlinearity and should be taken into account to predict the behavior of the system. In order to analyze correctly the stability of a given wave, we must not only consider the applied modulation Q, but also the modulation arising from the nonlinear terms and their combination modes in the simulations. Figure 2(a) shows the time evolution of carrier wave with wave vector $q=3\pi/32$

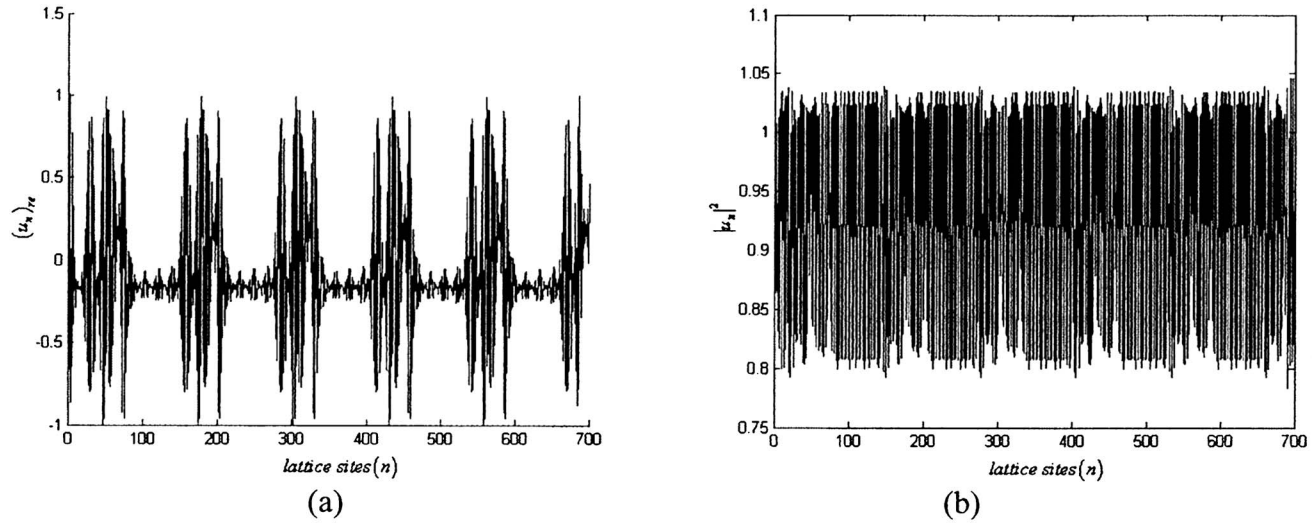

FIG. 5. Wave train $\alpha=3.0-3.25i$, $p=5.5-5.25i$, $C=-1.725+13.750i$, $\varepsilon=1$, $q=27\pi/64$, and a long-wavelength modulation $Q=7\pi/64$. (a) The amplitude of the wave function $|u_n|^2$ appears as a train of solitonlike objects. (b) The real part of the wave function $(u_n)_{re}$.

modulated by small amplitude wave ($\eta=u_0/100$), with wave vector $Q=\pm\pi/8$, for about 500 units of time. According to Fig. 1(a), the stability is predicted for wave with these wave vectors. This is effectively verified numerically in the log-linear plot of Fig. 2(a), in which none of the $3q$, $q\pm Q$, $q\pm 2Q$ satellite sidebands display any exponential growth. All these modulations which are not taken into account in the initial condition, display a constant amplitude. We also remark that their magnitude is less than the amplitude of the initial wave. Let us consider a wave with $q=\pi/32$ modulated at wave vector $Q=\pm 3\pi/16$. The corresponding point in the (q,Q) plane in Fig. 1(a) lies in the stability region. Figure 2(b) confirms this prediction of stability. However, we clearly see that the magnitude of the combination modes have increased but remain less than the magnitude of the initial wave. These two examples show that the analytical results leading to Eq. (23) give a correct estimation of the stability of a wave, provided that the wave vector of the modulation Q do not fail in the instability zone.

Figures 3(a) and 3(b) correspond to two predicted unstable cases. Figure 3(a) depicts a system with wave vector $q=5\pi/16$ modulated by wave vector $Q=\pm 3\pi/32$. We observe at the beginning that, the magnitude of the main carrier wave decreases exponentially before reaching a constant amplitude. While the magnitude of the combination modes $q-2Q$, $q\pm Q$ increases at the beginning. Notably, we observe that the magnitude of the combination mode $q-2Q$ is above the magnitude of the carrier wave. This feature is probably due to the fact that the system is subjected to the modulational instability. An interesting situation is displayed in Fig. 3(b) where we observe that the chaoticlike state mixing all wavelengths is obtained until $t=200$ units of time, instead of $t=25$ units of time as in Fig. 3(a). We also notice that while the magnitude of the carrier wave decreases, those of the combination modes increase until they reach a constant amplitude. Indeed, the magnitude of the combination modes $q-2Q$, $q\pm Q$ are all above the one of the carrier wave. This is the proof that at this time scale, the system is completely unstable. Although the linear-stability analysis neglects additional combination mode waves generated through wave-mixing process which, albeit small at the initial stage [see Figs. 2(a), 2(b), 3(a), and 3(b)], it can become significant and drive the system into a chaotic regime [see Fig. 3(b)] or their magnitude become higher [see Fig. 3(a) and Fig. 3(b)], if its modulation wave vector falls in an unstable domain. The physical parameters used for Figs. 2 and 3 are the same as those of Fig. 1.

B. Influence of the quintic nonlinearity on stability

If the parameters of the quintic nonlinearity are canceled ($c_r=c_m=0$), the model under study is the discrete cubic complex Ginzburg-Landau equation. It is well known from the literature that the cubic complex equation gives rise to unstable solution (as the equation includes a linear gain term, which makes the zero solution unstable, precluding stability of any solitary pattern). Let us illustrate it by another case with $q=\pi/8$ and for the modulation $Q=\pm\pi/16$. The physical parameters used here are $\alpha=1.5+0.725i$, $p=0.15-0.125i$, $c=-0.3+0.3i$, $\varepsilon=-0.25$. The (q,Q) point lies in the instability region. The system presents a chaotic behavior as it is well confirmed by the numerical simulation as shown in Fig. 4(a), which displays the time evolution of the Fourier component of the Q and $3q$ modulation. In this figure, we see that all the magnitude of the combination modes $(q,3q,q+Q,q+2Q)$ decreases exponentially then it increases, swiftly with the same shape. Figure 4(b) shows the complete Fourier spectrum of the full time evolution of waves on which we can observe that initially the amplitude of each mode increases slowly with increasing time. This result is in very good agreement with previous studies as those of Akhmediev and Ankiewicz who have shown that the cubic equation is known to lack stable solutions, except in very special cases when the solitons and the background are neutrally stable (when $\varepsilon=0$) [42]. Therefore, search for physically relevant models of the GL type that give rise to

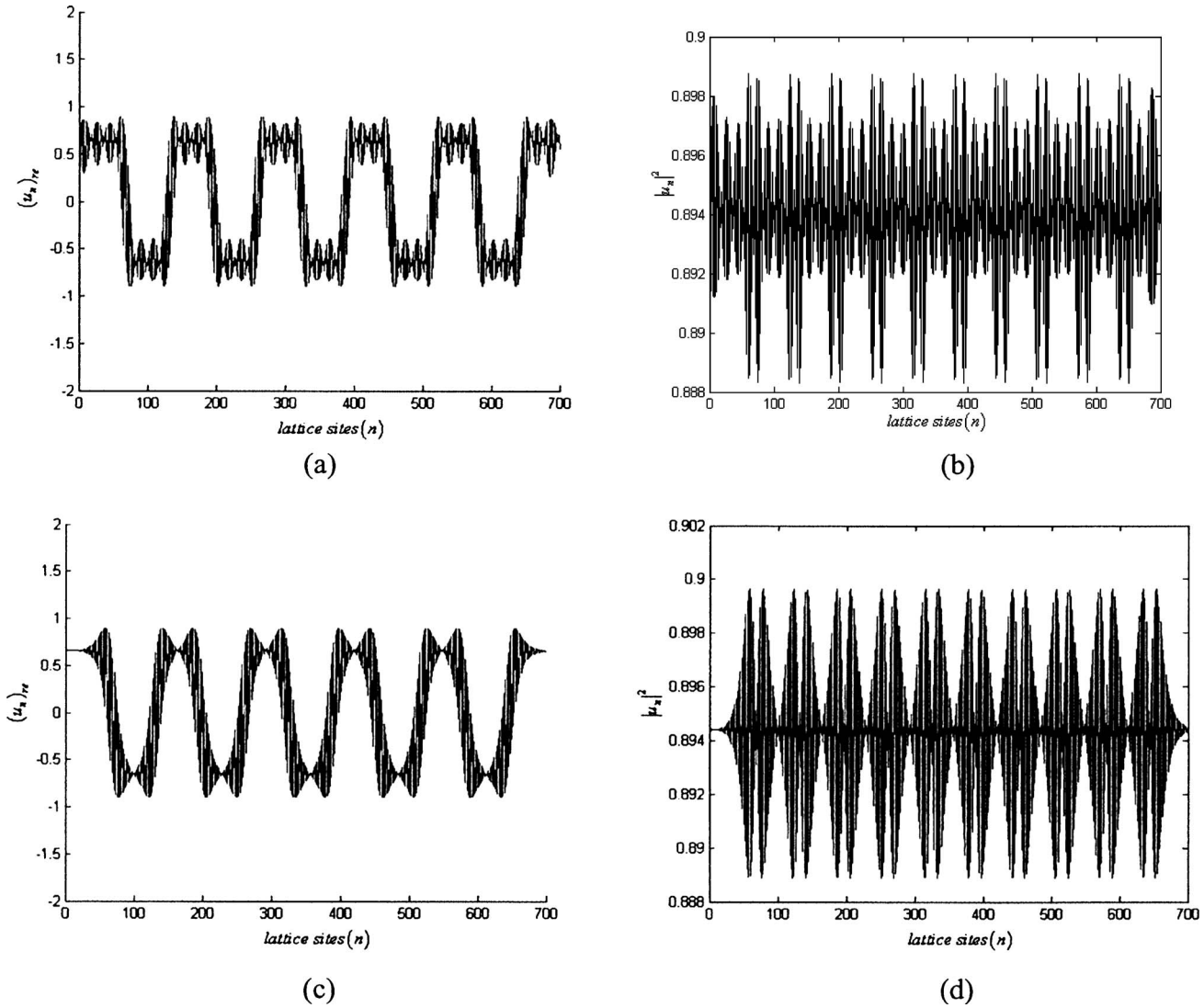

FIG. 6. Two-soliton-like shape $\alpha=3.0-3.25i$, $p=0.5-2.25i$, $C=-10.725+13.75$, $\varepsilon=1.0$, and for wave vectors $q=27\pi/64$, $Q=57\pi/64$. (a) The amplitude of the wave function $|u_n|^2$ appears as a train of solitonlike objects. (b) The real part of the wave function $(u_n)_{re}$.

stable pulses has attracted much attention. One possibility is to introduce a cubic-quintic GL equation with linear loss and cubic gain, nonlinear stability being provided by a quintic loss term. In this case we consider $c=-0.3+0.3i$. The result is immediate as it is shown in Fig. 4(c), after a chaoticlike state during the first 50 units of time; the amplitude of each mode stops its exponential increase. However, the system remains chaotic. The chaoticlike state mixing all wavelengths is obtained around $t=500$ units of time. The progressive build up of combination modes, due to nonlinear coupling induces wave interaction that are not included in our analysis and eventually all carrier waves evolve into a chaoticlike state where all possible wavelengths are present. Figure 4(d) illustrates this point. We present in Fig. 4(d) the complete Fourier spectrum of the time evolution of a carrier wave modulated by a wave vector that lies in the instability zone.

A recent study of Atai and Malomed [33] has also shown the usefulness of the quintic term in physical model. In their study, Atai and Malomed have shown that: the addition of the quintic term to the model makes the solitons very robust: simulating evolution of a strongly deformed pulse, they find that a larger part of its energy is *retained* in the process of its evolution into a soliton shape, only a small share of the energy being lost into radiation, which is opposite to what occurs in the usual BG model with cubic nonlinearity.

IV. WAVE PATTERN FORMATION IN THE DCCQGL EQUATION

Most studies related to discrete solitons are directed at conservative systems, i.e., those that preserve energy. There is an important difference between soliton solutions of Hamiltonian systems and autosoliton solutions in nonconservative systems [43]. In general, autosolitons are described by nonlinear partial differential equations of Ginzburg-Landau type. However, dissipative systems are more common in nature, so further studies on discrete dissipative systems are certainly still an open question. Recently these ideas have been applied to more complicated dissipative nonlinearities

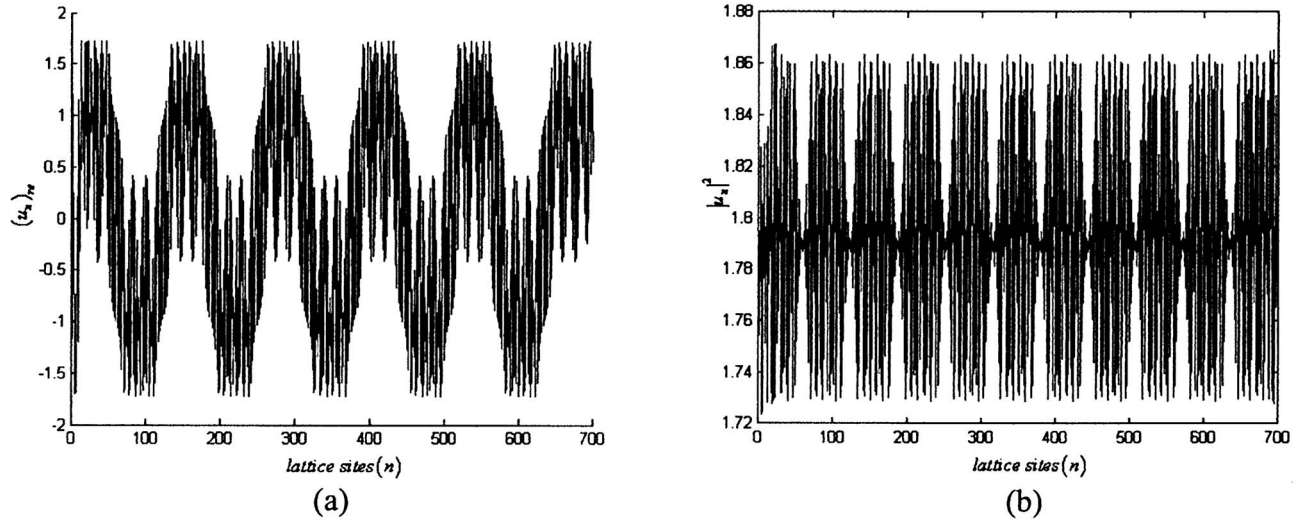

FIG. 7. Multisolitonlike shape $\alpha=1.0-0.25i$, $p=0.5-0.25i$, $C=-0.3+0.3i$, $\varepsilon=1.0$, $q=15\pi/32$, and $Q=15\pi/64$. (a) The amplitude of the wave function $|u_n|^2$ appears as a train of multisolitonlike objects. (b) The real part of the wave function $(u_n)_{re}$.

[44], and to higher-dimensional GL equation [45]. Moreover, it has been demonstrated some years ago that, the very nature of the GL system is such that can lead to extraordinary rich behavior ranging from chaos and pattern formation to self-localized solution or solitons. In the latter regime, the GL dissipative solitons (or autosolitons) are possible as a result of the interplay between linear and nonlinear gain, nonlinearity, and complex dispersion. Over the years, the soliton solutions of the Ginzburg-Landau equation and their underlying dynamics have been the subject of intense investigation. Such pulselike soliton states were first identified with in the context of the cubic GL mode and subsequently in the generalized quintic regime [25] and, typically, they represent chirped coherent structures (or one-dimensional defects) that are obtained through heteroclinic trajectories in the phase space of the stationary CGL equation. Closely related to the interplays between nonlinearity and dispersion is the process of MI. It is a symmetry-breaking instability so that a small perturbation on top of a constant amplitude background experiences exponential growth, and this leads to wave breakup in either space or time. These disintegrations have an envelope function with shape familiar from the theory of soliton-like objects. While MI is a crucial issue for solitons instability [14], it is also considered a precursor to solitons formation because it typically occurs in the same parameter region as that where solitons are observed [14].

In this section, we examine for a variety of equation parameters the nature of different wave patterns formation that may be raises up by a modulational instability processes in the DCCQGL equation. We then continue by using the definition of wave vector given above (i.e., $q=2\pi p/N$ and $Q=2\pi P/N$) for the carrier wave and the modulation wave. The system is now constituted of 700 sites and we use the initial condition given in Eq. (28). Now, we look to the feature of our initial modulated wave through the system. As a first example let us consider the parameters: $\alpha=3.0-3.25i$, $p=5.5-5.25i$, $C=-1.725+13.750i$, $\varepsilon=1$, $q=27\pi/64$, and a long-wavelength modulation $Q=7\pi/64$. According to Eq. (23), we expect the modulated wave to be unstable. One of the interesting phenomena we obtain is that, although the real or imaginary part of the wave displays an oscillating and breathing wave behavior, the amplitude of the wave displayed by wave motion is modulated in terms of a train of small-amplitude short waves. Each element of the train has the shape of a soliton object. To illustrate this point, we present in Figs. 5(a) and 5(b) at time $t=200$, the real part as well as the amplitude of the wave pattern displayed by these parameters. Next, for the parameters $\alpha=3.0-3.25i$, $p=0.5-2.25i$, $C=-10.725+13.75$, $\varepsilon=1.0$, and for wave vectors $q=27\pi/64$, $Q=57\pi/64$. The system is also supposed to be unstable for these values of parameters according to Eq. (23). We realize that there appears a modulation both in the amplitude and the real part as well as in the imaginary part of the wave function displayed by the wave motion. Here, the wave pattern displayed by the wave motion is constituted by an extended wave with an amplitude modulating into a train of double pulses amplitude. This phenomenon is depicted in Fig. 6. In Figs. 6(a) and 6(b), the real part of the function and its amplitude is plotted at time $t=200$, the wave degenerates into a train of double pulses. After a certain time, we observe that this wave degenerates now into a train of one pulse as shown in Figs. 6(c) and 6(d) at time $t=800$. As a last example, we consider as model parameters: $\alpha=1.0-0.25i$, $p=0.5-0.25i$, $C=-0.3+0.3i$, $\varepsilon=1.0$, $q=15\pi/32$, and $Q=15\pi/64$. The system is also supposed to be modulationally unstable in this case. It happens that the MI processes can lead to the generation of entities that have the appearance of multisolitonlike shapes with breathing motion. To illustrate this point, we have plotted in Figs. 7(a) and 7(b) the real part as well as the amplitude of the wave pattern displayed by the previous model parameters.

Finally, due to the discrete nature of the lattice, the difference in the shape of the waves generated by MI processes strongly depends on the value range of the wave vector carrier wave and the perturbation. They can be either extended or localized.

V. CONCLUSION

We have presented a detailed analysis of the MI's extended plane wave solutions of the discrete complex cubic-quintic Ginzburg-Landau equation. By employing the linear stability analysis, we have derived analytical expressions for the domain of existence as well as for the gain of MI of plane waves. Numerical calculations confirm the analytical results. We have shown that the stability conditions are qualitatively and quantitatively changed by the discreteness. We have also shown that the quintic nonlinearity is essential to stabilize the amplitude of the carrier wave and the one of combination modes. As in a recent experimental study on single-mode fibers [46], we have shown that the MI phenomenon can be exploited to generate a soliton train at high repetition rate.

ACKNOWLEDGMENT

Discussions with Yuri S. Kivshar of the Australian National University, Camberra, ACT 0200, Australia are appreciated.

[1] H. Ferddersen, in *Nonlinear Coherent Structures in Physics and Biology*, Lectures Notes in Physics (Spring-Verlag, Berlin, 1991).
[2] J. L. Rogerson and L. T. Wille, Phys. Rev. E **54**, R2193 (1996).
[3] R. Morandotti, D. Mandelik, Y. Silberberg, J. S. Aitchison, M. Sorel, D. N. Christodoulides, A. A. Sukhorukov, and Y. S. Kivhard, Opt. Lett. **29**, 2890 (2004).
[4] D. Gomila, R. Zambrini, and G.-L. Oppo, Phys. Rev. Lett. **92**, 253904 (2004); A. V. Yulin, D. V. Skyabin, and P. St. J. Russell, Opt. Express **13**, 3529 (2005).
[5] Y. Kuramoto, *Chemical Oscillations, Waves, and Turbulence* (Springer-Verlag, Berlin, 1984).
[6] C. M. de Sterke and J. E. Sipe, Phys. Rev. A **43**, 2467 (1991).
[7] E. A. Ultanir, G. I. Stegeman, and D. N. Christodoulides, Opt. Lett. **29**, 845 (2004).
[8] T. B. Benjamin and J. F. Feir, J. Fluid Mech. **27**, 417 (1967).
[9] V. I. Bespalov and V. I. Talanov, Zh. Eksp. Teor. Fiz. Pis'ma Red. **3**, 471 (1966) [JETP Lett. **3**, 307 (1966)].
[10] H. C. Yuen and B. M. Lake, in *Solitons in Action*, edited by K. Lonngren and A. Scott (Academic Press, New York, 1978).
[11] E. A. Kuznetsov, V. E. Zacharov, and A. M. Rubenchik, Phys. Rep. **142**, 103 (1986).
[12] C. Montes, O. Legrand, A. M. Rubenchik, and I. V. Relke, in *Nonlinear World* (World Scientific, Singapore, 1990), p. 1250.
[13] F. Abdullaev, S. Darmanyan, and P. Khabibullaev, *Optical Solitons* (Springer-Verlag, Heidelberg, 1993).
[14] G. P. Agrawal, *Nonlinear Fiber Optics* (Academic Press, San Diego, 2001).
[15] U. Peschel, O. Egorov, and F. Lederer, Opt. Lett. **29**, 1909 (2004).
[16] S. Darmanyan, I. Relke, and F. Lederer, Phys. Rev. E **55**, 7662 (1997).
[17] R. K. Dodd, J. C. Eilbeck, J. D. Gibbon, and H. C. Morris, *Solitons and Nonlinear Wave Equations* (Academic Press, London, 1984).
[18] M. C. Cross and P. C. Hohenberg, Rev. Mod. Phys. **65**, 851 (1993).
[19] M. Peyrard, T. Dauxois, H. Hoyet, and C. R. Willis, Physica D **68**, 104 (1993).
[20] D. N. Christodoulides and R. I. Joseph, Opt. Lett. **13**, 794 (1988). R. Marandotti, U. Peschel, J. S. Aitchison, H. S. Eisenberg, and Y. Silberberg, Phys. Rev. Lett. **83**, 2726 (1999).
[21] P. G. Kevrekidis, K. Ø. Rasmussen, and A. R. Bishop, Int. J. Mod. Phys. B **15**, 2833 (2000); J. P. Nguenang, M. Peyrard, A. J. Kenfack, and T. C. Kofané, J. Phys.: Condens. Matter **17**, 3083 (2005).
[22] Y. S. Kivshar and M. Peyrard, Phys. Rev. A **46**, 3198 (1992).
[23] V. M. Burlakov, S. A. Darmanyan, and V. N. Pyrkov, Phys. Rev. B **54**, 3257 (1996).
[24] I. S. Aranson and L. Kramer, Rev. Mod. Phys. **74**, 99 (2002).
[25] N. Akhmediev and A. Ankiewicz, *Solitons, Nonlinear Pulses and Beams* (Chapman and Hall, London, 1997).
[26] P. Manneville, *Dissipative Structures and Weak Turbulence* (Academic, San Diego, 1990).
[27] S. H. Strogatz and I. Stewart, Sci. Am. **269**, 102 (1993).
[28] E. A. Ultanir, G. I. Stegeman, and C. H. Lange, Opt. Lett. **30**, 531 (2005); K. Otsuka, *Nonlinear Dynamics in Optical Complex System* (KTK Scientific Publishers, Tokyo, 1999).
[29] H. Willaime, O. Cardoso, and P. Tabeling, Phys. Rev. Lett. **67**, 3247 (1991); A. Mohamadou, A. J. Kenfack, and T. C. Kofané, Phys. Rev. E **72**, 036220 (2005).
[30] J. F. Ravoux and P. Le Gal, Phys. Rev. E **58**, R5233 (1998).
[31] N. K. Efremidis and D. N. Christodoulides, Phys. Rev. E **67**, 026606 (2003).
[32] J. M. Soto-Crespo, N. Akhmediev, and A. Ankiewicz, Phys. Lett. A **314**, 126 (2003).
[33] J. Atai and B. A. Malomed, Phys. Lett. A **284**, 247 (2001).
[34] J. F. Ravoux, S. Le Dizès, and P. Le Gal, Phys. Rev. E **61**, 390 (2000).
[35] Y. S. Kivshar and B. Luther-Davies, Phys. Rep. **298**, 81 (1998).
[36] C. Kittel, *Introduction to Solid State Physics* (Wiley, New York, 1986).
[37] B. P. Anderson and M. A. Kasevich, Science **282**, 1686 (1998).
[38] A. Trombettoni and A. Smerzi, Phys. Rev. Lett. **86**, 2353 (2001).
[39] It is often useful to consider Eq. (1) in the so-called continuous limit at the base (edge) of the Brillouin zone, where it can be approximately written as
$$iU_z - i\epsilon' U \pm \alpha U_{xx} + p|U|^2 U + C|U|^4 U = 0 \quad \text{where } \epsilon' = \epsilon \pm 2\alpha_i.$$
[40] A. Jiotsa-Kenfack and T. C. Kofané, J. Phys. Soc. Jpn. **72**, 1800 (2003).
[41] C. G. Lange and A. C. Newell, SIAM J. Appl. Math. **27**, 441 (1974); F. B. Pelap and T. C. Kofané, Phys. Scr. **64**, 410 (2001).
[42] N. Akhmediev and A. Ankiewicz, in *Spatial Solitons*, edited by S. Trillo and W. E. Toruellas (Springer-Verlag, Berlin,

2001).
[43] N. N. Rosanov, *Spatial Hysteresis and Optical Patterns* (Springer-Verlag, Berlin, 2002).
[44] B. A. Malomed, A. G. Vladimirov, G. V. Khodova, and N. N. Rasanov, e-print nlinll.PS/0009011.
[45] V. Filho, F. Kh. Abdullaev, A. Gammal, and L. Tomio, Phys. Rev. A **63**, 053603 (2001).
[46] K. Tai, A. Hasegawa, and A. Tomita, Phys. Rev. Lett. **86**, 135 (1986).